Available online at www.sciencedirect.com

ScienceDirect

IFAC Papers Online CONFERENCE PAPER ARCHIVE

IFAC PapersOnLine 53-2 (2020) 7581–7586

Modelling and structure-preserving discretization of Maxwell's equations as port-Hamiltonian system ⋆

Gabriel Payen * **Denis Matignon** * **Ghislain Haine** *

* *ISAE-SUPAERO, Université de Toulouse, Toulouse, France*

Abstract: The modelling and discretization of the boundary controlled 3D Maxwell's equations as a port-Hamiltonian system is addressed. The proposed scheme, based on the Partitioned Finite Element Method (PFEM), originally proposed in Cardoso-Ribeiro et al. (2018), preserves the Dirac structure at the discrete level. Two types of damping phenomena are taken into account: Joule's effect, and a matrix-valued impedance at the boundary, both being preserved by PFEM, as presented in Serhani et al. (2019a).

Keywords: Maxwell's equations; port-Hamiltonian system; Partitioned Finite Element Method; Dirac structure; impedance; boundary control and observation.

1. INTRODUCTION

Nuclear fusion requires to control and confine a plasma heated at extreme temperature in a torus, with mainly the help of a magnetic field. A multi-physics model describing a plasma must take into account electromagnetism, mechanics, hydrodynamics and thermodynamics laws, which are highly coupled with each other, see *e.g.* Vu (2014); Vu et al. (2016). The port-Hamiltonian approach seems to be adapted to describe this complex multi-physics system. Indeed, port-Hamiltonian systems (pHs), introduced a few decades ago, see *e.g.* van der Schaft and Maschke (2002); Duindam et al. (2009) for the extension to infinite-dimensional setting, are a powerful tool to represent complex physical systems, based on exchanges of energy between their components. Furthermore, pHs are strongly related to Dirac structure, allowing for easy-to-state power-preserving interconnections.

The structure-preserving discretization of such types of distributed parameters systems is indeed a very interesting way to perform the numerical simulation of complex systems, allowing for the preservation of the different physical phenomena at stake. An ever-growing literature now exists on this important subject. We refer to Eberard et al. (2007) for the interconnections of discretized port-Hamiltonian systems; see also the recent book Kotyczka (2019) and the many references therein.

Recently, pHs modelling for electromagnetism has been investigated by Vu et al. in Vu (2014), Vu et al. (2012); see also Farle et al. (2013) for an interesting numerical method using differential forms with worked out examples in 1D.

The main aim of this paper is to apply the Partionned Finite Elements Method (PFEM), see Cardoso-Ribeiro et al. (2018, 2019), to a simplified 3D electromagnetic model: indeed, this example will complete previous applications on membranes and plates, see *e.g.* Serhani et al. (2019b); Brugnoli et al. (2019a,b), and show how PFEM can provide a 3D structure-preserving way to discretize pHs, in the case of a PDE system based on **curl** operators and with a vector-valued control at the boundary; on the numerical side, the complete and efficient framework of finite elements for electromagnetism can be used for simulation, see e.g Monk (2003).

The novelties of this work, see Payen et al. (2018), are the following: first, the system is governed by (**curl** , $-$**curl**) operators instead of (div , **grad**) operators for membranes, or of (**Div** , **Grad**) operators for plates; second, the system is fully 3D instead of 2D for the previous applications of the partitioned finite element method; finally, the boundary fields are vector fields and not scalar fields, which leads to extra difficulties.

The paper is organized as follows: the continuous boundary controlled Maxwell's equations are recalled in § 2; then a structure-preserving discretization of the system is presented in § 3, and simulation results are provided to illustrate its efficiency to preserve the power balance satisfied by the total electromagnetic energy at the discrete level. An application is then detailed in § 4: a matrix-valued impedance at the boundary is taken into account and discretized in a structure-preserving manner to tackle the difficult problem of simulation of boundary dissipation. Finally conclusions are drawn and future work is presented in § 5.

2. CONTINUOUS MODEL

The aim of this section is to recast Maxwell's equations as a port-Hamiltonian system in § 2.1, taking into account internal dissipation due to Joule's effect, § 2.2, and examine some ideal boundary conditions in § 2.3. Indeed these

⋆ This work is supported by the project n° ANR-16-CE92-0028, entitled *Interconnected Infinite-Dimensional systems for Heterogeneous Media*, INFIDHEM, financed by the French National Research Agency (ANR) and the Deutsche Forschungsgemeinschaft (DFG). Further information is available at `https://websites.isae-supaero.fr/infidhem/the-project`.

10.1016/j.ifacol.2020.12.1355

different steps will prove necessary in order to apply a structure-preserving discretization method in § 3.

All the definitions and identities used below are recalled in Appendices A and B.

2.1 Dynamical model and energy balance

The Hamiltonian of the system is the total electromagnetic energy, given by:

$$\mathcal{E}_{em}(\mathbf{D},\mathbf{B}) := \frac{1}{2}\int_\Omega \frac{\mathbf{D}\cdot\mathbf{D}}{\epsilon} + \frac{\mathbf{B}\cdot\mathbf{B}}{\mu}. \tag{1}$$

Electric and magnetic *inductions* $\mathbf{D}$, $\mathbf{B}$ are chosen as energy variables; then computing the variational derivatives of the Hamiltonian $\mathcal{E}_{em}$ with respect to them, the electric and magnetic *fields*:

$$\mathbf{E} := \delta_{\mathbf{D}}\mathcal{E}_{em}\,, \qquad \mathbf{H} := \delta_{\mathbf{B}}\mathcal{E}_{em}\,,$$

naturally appear as co-energy variables. The constitutive laws linking them involve the electric permittivity $\epsilon(\mathbf{x})$ and the magnetic permeability $\mu(\mathbf{x})$, and read:

$$\mathbf{D} = \epsilon\mathbf{E}, \qquad \text{and} \qquad \mathbf{B} = \mu\mathbf{H}\,. \tag{2}$$

With these notations at hand, the two dynamical Maxwell's equations (Maxwell-Ampère and Maxwell-Faraday) can be written as:

$$\partial_t\mathbf{D} = \mathbf{curl}\ \mathbf{H} - \mathbf{J}\,, \tag{3}$$

$$\partial_t\mathbf{B} = -\mathbf{curl}\ \mathbf{E}\,. \tag{4}$$

Moreover, $\mathbf{J}$ stands for the total inner distributed current: Ohm's law states that $\mathbf{J} = \eta^{-1}\mathbf{E}$, with $\eta(\mathbf{x})$ the resistivity, responsible of the so-called Joule's effect; this latter relation can be seen as a third constitutive relation. As such, the dynamical system is closed.

Remark 1. In this work, following the example of van der Schaft and Maschke (2002), we do not consider the two other static equations explicitely, namely Maxwell-Gauß div $\mathbf{D} = \rho$ in presence of a charge density ρ, or Maxwell-flux div $\mathbf{B} = 0$. Both these equations add algebraic constraints on the solutions which need to be taken in account when solving the problem ; for short, if the initial data fullfill these constraints, they will be satisfied along the solutions of the infinite-dimensional dynamical system, see e.g. Weiss and Staffans (2013) for a detailed discussion on this point.

Energy balance Using definition (1), dynamic equations (3)–(4) and identity (A.1), one can compute the electromagnetic power as follows:

$$\begin{aligned}\frac{d\mathcal{E}_{em}}{dt} &= \int_\Omega \mathbf{E}\cdot\partial_t\mathbf{D} + \mathbf{H}\cdot\partial_t\mathbf{B}\,,\\ &= \int_\Omega (\mathbf{E}\cdot\mathbf{curl}\ \mathbf{H} - \mathbf{H}\cdot\mathbf{curl}\ \mathbf{E}) - \int_\Omega \mathbf{E}\cdot\mathbf{J}\,,\\ &= -\int_\Omega \mathrm{div}\ (\mathbf{E}\wedge\mathbf{H}) - \int_\Omega \mathbf{E}\cdot\mathbf{J}\,,\\ &= -\int_{\partial\Omega} \mathbf{\Pi}\cdot\mathbf{n} - \int_\Omega \mathbf{E}\cdot\mathbf{J}\,,\end{aligned} \tag{5}$$

where $\mathbf{\Pi} := \gamma(\mathbf{E}\wedge\mathbf{H})$ defined on the boundary $\partial\Omega$ is known as Poynting vector. Thus, the loss of electromagnetic energy comes from the flux of the Poynting vector across the boundary $\partial\Omega$, and the distributed power in the domain Ω, with density $\mathbf{E}\cdot\mathbf{J} = \eta\|\mathbf{J}\|^2 = \eta^{-1}\|\mathbf{E}\|^2 \geq 0$, which is actually Joule's effect; this energy is lost in the thermal domain, see *e.g.* Vu et al. (2016).

For the boundary term, following Appendix B, there are several ways of defining collocated boundary inputs and outputs, see (B.1); in the sequel we will choose electric control (through voltage V_{loop}) $\mathbf{u}_\partial := \gamma_\tau(\mathbf{E})$ the tangential trace of the electric field, and magnetic observation (through plasma current $\mathbf{I_p}$) $\mathbf{y}_\partial := \mathbf{n}\wedge\gamma(\mathbf{H})$, the rotated tangential trace of the magnetic field. Indeed, one of the stability issues in tokamaks lies in the current measured at the boundary of the reactor: called *plasma current* and denoted $\mathbf{I_p}$, it needs to be controlled; a control which is convenient to apply is a voltage V_{loop} at the boundary: see Vu et al. (2016) for more details about the physical meaning of this choice. For other applications, other choices can be made (the power product $\mathbf{u}_\partial\cdot\mathbf{y}_\partial$ must equal the normal component of the Poynting vector).

Now in § 2.2, we discuss how this boundary controlled and observed infinite-dimensional system can be recast into a Stokes-Dirac structure, while in § 2.3 a focus is given on a closed systems, namely the perfect conductor.

2.2 Flows-efforts formulation and Stokes-Dirac structure

Following e.g. Duindam et al. (2009), the electromagnetic fields and the dissipation can be embedded together into an extended Stokes-Dirac structure, making use of extra *dissipation* ports $\mathbf{e_J} := \mathbf{J}$, and $\mathbf{f_J} := \mathbf{E}$ related through a closure relation $\mathbf{e_J} = \eta^{-1}\mathbf{f_J}$.

Let us define the electric effort by $\mathbf{e_e} := \mathbf{E}$, the magnetic effort by $\mathbf{e_m} := \mathbf{H}$ and the boundary effort as $\mathbf{e}_\partial := \mathbf{E}_\tau = (\mathbf{n}\wedge\mathbf{E})\wedge\mathbf{n} = \mathbf{u}_\partial$, and then $(\overrightarrow{\mathbf{e}}, \mathbf{e}_\partial) = (\mathbf{e_e}, \mathbf{e_m}, \mathbf{e_J}, \mathbf{e}_\partial) \in \mathcal{E}$, the effort space. Let us define the electric flow by $\mathbf{f_e} := \partial_t\mathbf{D}$, the magnetic flow by $\mathbf{f_m} := \partial_t\mathbf{B}$ and the boundary flow as $\mathbf{f}_\partial := (\mathbf{H}\wedge\mathbf{n}) = -\mathbf{y}_\partial$, and then $(\overrightarrow{\mathbf{f}}, \mathbf{f}_\partial) = (\mathbf{f_e}, \mathbf{f_m}, \mathbf{f_J}, \mathbf{f}_\partial) \in \mathcal{F}$, the flow space. These flows and efforts are related through:

$$\begin{pmatrix}\mathbf{f_e}\\ \mathbf{f_m}\\ \mathbf{f_J}\end{pmatrix} = \begin{pmatrix}0 & \mathbf{curl} & -I\\ -\mathbf{curl} & 0 & 0\\ I & 0 & 0\end{pmatrix}\begin{pmatrix}\mathbf{e_e}\\ \mathbf{e_m}\\ \mathbf{e_J}\end{pmatrix}, \tag{6}$$

which can be shortened into $\overrightarrow{\mathbf{f}} = \mathcal{J}\overrightarrow{\mathbf{e}}$. Obviously, the matrix-valued differential operator $\mathcal{J}$ is formally skew-symmetric, since the curl operator is formally symmetric, $\mathbf{curl}^{\,*} = \mathbf{curl}$.

This nice structure in (6) must be complemented with *closure (or constitutive) relations* for well-posedness, namely three of them since three lines are involved in (6). Indeed, we already have mentionned them: $\mathbf{e_e} = \epsilon^{-1}\mathbf{D}$, $\mathbf{e_m} = \mu^{-1}\mathbf{B}$, and $\mathbf{e_J} = \eta^{-1}\mathbf{f_J}$.

With the boundary ports $(\mathbf{e}_\partial, \mathbf{f}_\partial)$, we can now make use of the *formal skew-symmetry* of the structure operator appearing in (6) to conclude that equation (5) leads to:

$$\langle(\overrightarrow{\mathbf{f}}, \mathbf{f}_\partial), (\overrightarrow{\mathbf{e}}, \mathbf{e}_\partial)\rangle_{\mathcal{F},\mathcal{E}} = 0\,, \tag{7}$$

which is equivalent to the fact that flows and efforts lay in an underlying Stokes-Dirac structure $\mathcal{D} \subset \mathcal{F}\times\mathcal{E}$ endowed with the appropriate bilinear symmetrized pairing. In a more concrete way, (7) reads:

$$\int_\Omega \overrightarrow{\mathbf{f}}\cdot\overrightarrow{\mathbf{e}} + \int_{\partial\Omega} \mathbf{e}_\partial\cdot\mathbf{f}_\partial = 0\,.$$

Thus, denoting $\mathcal{P}_J := \int_\Omega \mathbf{e_J} \cdot \mathbf{f_J} = \int_\Omega \eta \|\mathbf{e_J}\|^2 \geq 0$, the power dissipated thanks to Joule's effect, it is possible to decompose:

$$\frac{d\mathcal{E}_{em}}{dt} = -\int_{\partial\Omega} \mathbf{e}_\partial \cdot \mathbf{f}_\partial - \mathcal{P}_J\,,$$

with the help of the boundary ports.

2.3 Some ideal boundary conditions for the closed system

Suppose there is no internal dissipation $\mathcal{P}_J = 0$, meaning either that $\eta = 0$ or $\eta^{-1} = 0$, then the losses come from the boundary only, as shown by balance (5).

A classical model consists in considering *perfect conductor* boundary conditions:

$$\gamma(\mathbf{E}) \wedge \mathbf{n} = 0, \qquad \gamma(\mathbf{B}) \cdot \mathbf{n} = 0. \tag{8}$$

Indeed, with (8) and the help of Appendix B, one can compute $\mathbf{\Pi} \cdot \mathbf{n} = 0$, hence the closed system proves conservative: $\frac{d\mathcal{E}_{em}}{dt} = 0$.

3. PARTITIONED FINITE ELEMENTS METHOD (PFEM)

The goal of this section is to apply a structure-preserving discretization method to the continuous Maxwell's equations: the weak formulation of the system is presented in § 3.1, a Dirac structure is recovered in § 3.2, and a discussion on the compatible finite elements to be used in practise is carried out in § 3.3.

3.1 Weak formulation

PFEM proceeds in 3 steps:

(1) apply Stokes' formula on one of the two equations written in weak form, as to make the boundary control of interest appear,
(2) apply a weak formulation to the constitutive equations also,
(3) as test functions, choose scalar-valued or vector-valued finite-elements that prove compatible with the functional spaces of interest.

Let us give the results of the main steps on our extended system.

Structure in weak form Elements of the same nature should share similar properties: the viewpoint adopted in this work and used in Section 3.4, consists in discretizing electric variables in one basis, and magnetic variables in another basis (*a priori*) [1]. Then, it is natural to consider two different Hilbert spaces $\mathcal{H}_e$ and $\mathcal{H}_m$ which will be discussed in § 3.3. The weak formulation reads:

$$\begin{aligned}
\int_\Omega \mathbf{\Phi^e} \cdot \partial_t \mathbf{D} &= \int_\Omega \mathbf{\Phi^e} \cdot \mathbf{curl}\ \mathbf{H} - \int_\Omega \mathbf{\Phi^e} \cdot \mathbf{J}\,,\\
\int_\Omega \mathbf{\Phi^m} \cdot \partial_t \mathbf{B} &= -\int_\Omega \mathbf{\Phi^m} \cdot \mathbf{curl}\ \mathbf{E}\,,\\
\int_\Omega \mathbf{\Phi^e} \cdot \mathbf{f_J} &= \int_\Omega \mathbf{\Phi^e} \cdot \mathbf{E}\,, \quad \forall \mathbf{\Phi^e}, \mathbf{\Phi^m} \in \mathcal{H}_e \times \mathcal{H}_m\,.
\end{aligned}$$

[1] However, as discussed in Section 3.3, another viewpoint would consist in discretizing *inductions* on the one hand, and *fields* on the other hand.

One can integrate the second line by parts, and obtain:

$$\begin{aligned}
\int_\Omega \mathbf{\Phi^e} \cdot \partial_t \mathbf{D} &= \int_\Omega \mathbf{\Phi^e} \cdot \mathbf{curl}\ \mathbf{H} - \int_\Omega \mathbf{\Phi^e} \cdot \mathbf{J}\,,\\
\int_\Omega \mathbf{\Phi^m} \cdot \partial_t \mathbf{B} &= -\int_\Omega \mathbf{curl}\ \mathbf{\Phi^m} \cdot \mathbf{E} - \int_{\partial\Omega} (\mathbf{\Phi^m} \wedge \mathbf{n}) \cdot \mathbf{E}\,,\\
\int_\Omega \mathbf{\Phi^e} \cdot \mathbf{f_J} &= \int_\Omega \mathbf{\Phi^e} \cdot \mathbf{E}\,, \quad \forall \mathbf{\Phi^e}, \mathbf{\Phi^m} \in \mathcal{H}_e \times \mathcal{H}_m\,.
\end{aligned}$$

Let us consider conforming finite elements spaces $\overline{H_e} \subset \mathcal{H}_e$ and $\overline{H_m} \subset \mathcal{H}_m$. A space $\overline{H_\partial} \subset \mathcal{H}_\partial$ is also needed for boundary variables. These finite-dimensional spaces are spanned by bases denoted as follows:

$$\begin{aligned}
\mathrm{span}((\mathbf{\Phi^e_i})_{i=1\ldots N_e}) &= \overline{H_e}\,,\\
\mathrm{span}((\mathbf{\Phi^m_j})_{j=1\ldots N_m}) &= \overline{H_m}\,,\\
\mathrm{span}((\mathbf{\Psi^\partial_k})_{k=1\ldots N_\partial}) &= \overline{H_\partial}\,.
\end{aligned}$$

Variables are approximated on these bases as follows:

$$\mathbf{D}(\mathbf{x}, t) \approx \mathbf{D}^d(\mathbf{x}, t) := \sum_{i=1}^{N_e} D_j(t) \mathbf{\Phi^e_i}(\mathbf{x}) = \mathbf{\Phi^e}^\top(\mathbf{x})\, \underline{D}(t),$$

and similarly for all the other variables, in their respective basis. The unknown now is the $N_e \times 1$ time-dependent vector $\underline{D}(t) = (D_1(t), \ldots D_{N_e}(t))^\top$; the matrix $\mathbf{\Phi^e}(\mathbf{x})$ being space dependent, and of size $N_e \times 3$.

Thus, plugging these approximations into the second weak form reads, $\forall i = 1..N^e, j = 1..N^m$:

$$\begin{aligned}
\int_\Omega \sum_{j=1}^{N_e} \mathbf{\Phi^e_i} \cdot \mathbf{\Phi^e_j} \partial_t D_j(t) &= \int_\Omega \sum_{j=1}^{N_m} \mathbf{\Phi^e_i} \cdot \mathbf{curl}\ \mathbf{\Phi^m_j} H_j(t)\,,\\
&\quad - \int_\Omega \sum_{j=1}^{N_e} \mathbf{\Phi^e_i} \cdot \mathbf{\Phi^e_j} J_j(t)\,,\\
\int_\Omega \sum_{j=1}^{N_b} \mathbf{\Phi^m_k} \cdot \mathbf{\Phi^m_j} \partial_t B_j(t) &= -\int_\Omega \sum_{j=1}^{N_e} \mathbf{\Phi^e_j} \cdot \mathbf{curl}\ \mathbf{\Phi^m_k} E_j(t),\\
&\quad - \int_{\partial\Omega} \sum_{l=1}^{N_\partial} (\mathbf{\Phi^m_k} \wedge \mathbf{n}) \cdot \mathbf{\Psi^\partial_l} E^\partial_l(t)\,,\\
\int_\Omega \sum_{j=1}^{N_e} \mathbf{\Phi^e_i} \cdot \mathbf{\Phi^e_j} f_J(t) &= \int_\Omega \sum_{j=1}^{N_e} \mathbf{\Phi^e_i} \cdot \mathbf{\Phi^e_j} E_j(t).
\end{aligned}$$

Let us introduce the following matrices:

$$\begin{aligned}
(M_e)_{i,j} &= \langle \mathbf{\Phi^e_i}, \mathbf{\Phi^e_j} \rangle_{L^2(\Omega)} \quad \text{of size } N_e \times N_e\,,\\
(M_m)_{i,j} &= \langle \mathbf{\Phi^m_i}, \mathbf{\Phi^m_j} \rangle_{L^2(\Omega)} \quad \text{of size } N_m \times N_m\,,\\
(M_\partial)_{i,j} &= \langle \mathbf{\Psi^\partial_i}, \mathbf{\Psi^\partial_j} \rangle_{L^2(\partial\Omega)} \quad \text{of size } N_\partial \times N_\partial\,,\\
(C)_{i,j} &= \langle \mathbf{\Phi^e_i}, \mathbf{curl}\ \mathbf{\Phi^m_j} \rangle_{L^2(\Omega)} \quad \text{of size } N_e \times N_m\,,\\
(T)_{i,j} &= \langle (\mathbf{\Phi^m_i} \wedge \mathbf{n}), \mathbf{\Psi^\partial_j} \rangle_{L^2(\partial\Omega)} \quad \text{of size } N_m \times N_\partial\,.
\end{aligned}$$

With these compact notations at hand, the finite-dimensional system with input $\underline{u}_\partial(t) := \underline{E}_\partial(t)$ now reads:

$$\begin{pmatrix} M_e\, \underline{\dot{D}} \\ M_m\, \underline{\dot{B}} \\ M_e\, \underline{f_J} \end{pmatrix} = \begin{pmatrix} 0 & C & -M_e \\ -C^\top & 0 & 0 \\ M_e & 0 & 0 \end{pmatrix} \begin{pmatrix} \underline{E} \\ \underline{H} \\ \underline{J} \end{pmatrix} - \begin{pmatrix} 0 \\ T \\ 0 \end{pmatrix} \underline{u}_\partial\,, \tag{9}$$

with conjugated output:

$$M_\partial\, \underline{y}_\partial = -\begin{pmatrix} 0 & T^\top & 0 \end{pmatrix} \begin{pmatrix} \underline{E} \\ \underline{H} \\ \underline{J} \end{pmatrix}. \tag{10}$$

The square matrix J^d appearing in (9) linking efforts and flows is clearly skew symmetric.

Remark 2. It is an interesting exercice to prove that $\underline{y}_\partial(t)$ defined in (10) does indeed correspond to the out-

put $\mathbf{y}_\partial(\mathbf{x},t) := \mathbf{n}(\mathbf{x}) \wedge \mathbf{H}(\mathbf{x},t)$ discretized on the family $\{\mathbf{\Psi}^\partial_\mathbf{j}(\mathbf{x})\}_{1\leq j\leq N_\partial}$ at the boundary.

Constitutive relations in weak form The three constitutive equations at the continuous level can also be spatially averaged, and written in finite-dimensional form:

$$\begin{aligned} \langle\epsilon^{-1}\rangle\,\underline{D} &= M_e\,\underline{E}, & \langle\epsilon^{-1}\rangle_{i,j} &:= \langle\epsilon^{-1}\mathbf{\Phi}^\mathbf{e}_\mathbf{i}, \mathbf{\Phi}^\mathbf{e}_\mathbf{j}\rangle_{L^2(\Omega)}\,,\\ \langle\mu^{-1}\rangle\,\underline{B} &= M_m\,\underline{H}, & \langle\mu^{-1}\rangle_{i,j} &:= \langle\mu^{-1}\mathbf{\Phi}^\mathbf{m}_\mathbf{i}, \mathbf{\Phi}^\mathbf{m}_\mathbf{j}\rangle_{L^2(\Omega)}\,,\\ \langle\eta^{-1}\rangle\,\underline{f_J} &= M_e\,\underline{e_J}, & \langle\eta^{-1}\rangle_{i,j} &:= \langle\eta^{-1}\mathbf{\Phi}^\mathbf{e}_\mathbf{i}, \mathbf{\Phi}^\mathbf{e}_\mathbf{j}\rangle_{L^2(\Omega)}\,. \end{aligned} \tag{11}$$

Remark 3. Note that when the parameter are uniform in space, the previous averaged equations in weak form simplify into $\underline{D} = \epsilon\,\underline{E}$, $\underline{B} = \mu\,\underline{H}$ and $\underline{J} = \eta^{-1}\,\underline{E}$, as for the constitutive relations in the continuous case!

Now, thanks to the 3 above constitutive relations, the finite-dimensional dynamical system (9)–(10) is closed, and ready for numerical simulation.

3.2 Recovering a Dirac structure

It enjoys some very nice propery, indeed, the Stokes-Dirac structure of the continuous system has been inherited at the discrete level, giving rise to a Dirac structure in dimension $N_e \times N_m \times N_e$, the inputs and outputs being of dimension N_∂.

The discrete electromagnetic energy is defined as follows:

$$\begin{aligned} \mathcal{E}^d_{em}(t) &:= \mathcal{E}_{em}(D^d(t), B^d(t))\,,\\ &= \mathcal{E}_{em}(\mathbf{\Phi^e}^\top(\mathbf{x})\,\underline{D}(t), \mathbf{\Phi^m}^\top(\mathbf{x})\,\underline{B}(t))\,,\\ &= \frac{1}{2}\underline{D}(t)^\top\langle\epsilon^{-1}\rangle\,\underline{D}(t) + \frac{1}{2}\underline{B}(t)^\top\langle\mu^{-1}\rangle\,\underline{B}(t)\,. \end{aligned}$$

At the discete level, the following energy balance can be recovered thanks to a straightforward computation, making use both of the skew-symmetry of the matrix J^d in (9), and of the symmetry of the matrices involved in the discrete constitutive relations (11):

$$\begin{aligned} \frac{d\mathcal{E}^d_{em}(t)}{dt} &= -\underline{E}(t)^\top\langle\eta^{-1}\rangle\,\underline{E}(t) + \underline{y}_\partial(t)^\top M_\partial\,\underline{u}_\partial(t)\,,\\ &\leq (\underline{u}_\partial(t), \underline{y}_\partial(t))_{M_\partial}\,, \end{aligned}$$

meaning that the open dynamical system is passive, or the closed dynamical system is lossy.

3.3 Compatible Finite Elements

The final step concerns the effective implementation of PFEM. As mentionned in Farle et al. (2013), either $H_{\mathrm{div}} \cap H_{\mathbf{curl}}$ -conforming finite elements might be needed, or a careful analysis has to be done for non-conforming finite element to ensure good results.

An easy choice for conforming finite elements is the P^k-Lagrange finite elements (with $k \geq 1$), since they are $(H^1)^3 \subset H_{\mathrm{div}} \cap H_{\mathbf{curl}}$. However, this raises a new difficulty to impose the control at the boundary properly. Indeed, Raviart-Thomas (H_{div} -conforming but not $H_{\mathbf{curl}}$) or Nédélec ($H_{\mathbf{curl}}$ -conforming but not H_{div}) finite elements lead to *e.g.* $(\mu\mathbf{H})\cdot\mathbf{n}$ (normal) or *e.g.* $\mathbf{E}\wedge\mathbf{n}$ (tangential) boundary conditions respectively, whereas P^k-Lagrange elements induce a stronger imposition with three degrees of freedom (a priori neither normal nor tangential). This might be solved by a computation on the boundary of the three components of the control u, in the local basis given by $\mathbf{n}$, to ensure that the values imposed to each H^1 component lead to the desired boundary condition. In our opinion, this solution might be expensive and sources of numerical errors which are difficult to control in an arbitrary domain Ω.

Another difficulty, independent of the previous one, concerns the constraints on the divergence of each field. However, in the conforming case, a mixed formulation with Lagrange multipliers (taking care about the necessary *inf-sup* condition) would do the job. Fortunately, the use of known finite elements for **curl** − div systems such as the Raviart-Thomas-Nédélec finite elements, see Monk (2003), based on the celebrated de Rham cohomology and Hodge-Helmholtz decomposition of $(L^2)^3$, leads us to consider the extension of PFEM to the case where flows and efforts are not approximated in the same basis: **D** and **B** in an H_{div} -conforming space, as *inductions*, and **H** and **E** in an $H_{\mathbf{curl}}$ -conforming space, as *fields*. Note that this is thankfully coherent with the tangential controls proposed in § 4 on **H** or **E** below. The initial drawback is then postponed to the consistent discretization of the consistutive relations $\mathbf{D} = \epsilon\mathbf{E}$ and $\mathbf{B} = \mu\mathbf{H}$, which then possibly induce non-square matrices in (11). Note that this is also consistent with the exterior derivative approach developped *e.g.* in Farle et al. (2013).

Finally, the system (9)–(10)–(11) to solve is a Differential Algebraic Equation (DAE) in its present form. This kind of port-Hamiltonian Differential Algebraic Equations (pHDAE), although natural, require the use of specific time schemes to preserve the port-Hamiltonian structure: this is an active topic of research, see *e.g.* Beattie et al. (2018), but not the purpose of this work. Nevertheless, following previous works on application of PFEM to hyperbolic systems (see *e.g.* Brugnoli et al. (2019a) and Serhani et al. (2019a)), we can overcome this difficulty quite easily, by rewritting the system in its *co-energy formulation*. It consists in substituting **D**, **B** and **J** thanks to the constitutive relations (2) and Joule's effect. Note that it proves equivalent to do this at the continuous level, or to do it after discretization, as soon as $\overline{H_m}$ and $\overline{H_e}$ have been wisely chosen (*i.e.* with *weighted* finite elements, see Haine et al. (2020) for a detailed discussion on the wave equation). In this approach, we end up with two coupled PDEs in **E** and **H**, without any constitutive relations to discretize anymore. The application of PFEM then leads to an Ordinary Differential Equation (ODE), for which usual symplectic time schemes can be used. However, this does not solve the previsouly stated issue about the divergence of the inductions, as shall be seen in the following section.

3.4 Simulations

In this section, an illustration of the structure-preserving scheme of Section 3.1 is provided, with Joule's effect and voltage boundary control: we solve (9)–(10)–(11).

To avoid the difficulties induced by DAE, we apply PFEM on the *co-energy formulation*, as explained above. Thus, the system to be solved now reads:

$$\begin{pmatrix}\langle\epsilon\rangle & 0\\ 0 & \langle\mu\rangle\end{pmatrix}\begin{pmatrix}\dot{\underline{E}}\\ \dot{\underline{H}}\end{pmatrix} = \left(\begin{pmatrix}0 & C\\ -C^\top & 0\end{pmatrix} - \begin{pmatrix}\langle\eta^{-1}\rangle & 0\\ 0 & 0\end{pmatrix}\right)\begin{pmatrix}\underline{E}\\ \underline{H}\end{pmatrix} - \begin{pmatrix}0\\ T\end{pmatrix}\underline{u}_\partial,$$

where $\langle\epsilon\rangle$ and $\langle\mu\rangle$ are defined as in (11).

We perform a first simulation on a *torus*, making use of FreeFem++ (Hecht (2012)).

We choose Nédélec finite elements of order 1 for $\mathbf{E}$ and $\mathbf{H}$, known to be $H_{\mathbf{curl}}$ -conforming. To be consistent with the tangential trace of Nédélec finite elements (see *e.g.* Monk (2003)), the boundary control and observation variables are approximated by discontinuous P^1-Lagrange elements *on the surface of the torus*. The number of degrees of freedom (dof) for $\underline{E}$ and $\underline{H}$ is 15,144, while the number of dof at the boundary is 11,436. The time integration is performed *via* a Crank-Nicolson scheme with a time step $\Delta t = 10^{-3}$ over the time interval $[0, 3]$. The initial data (divergence-free) and control are taken to be compatible at the initial time $t = 0$, as required. For sake of simplicity in this first attempt, $\epsilon = \mu = \eta = 1$.

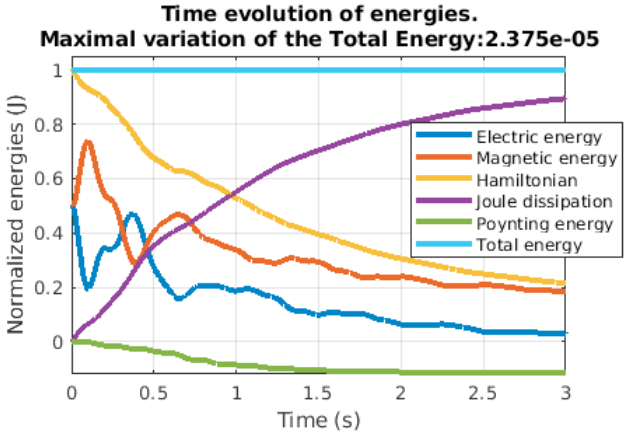

Fig. 1. Normalized energies versus time (Torus).

We can appreciate on Fig. 1 the precision of the power balance, despite the coarse mesh and low order in space and time. The *total energy*, representing the sum of the Hamiltonian, the Joule's dissipation, and the energy supplied to (or took from) the system *via* the control, is indeed very stable with a maximal variation of 10^{-5}.

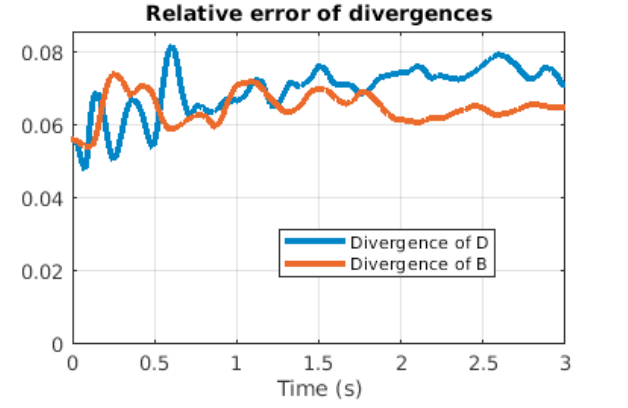

Fig. 2. L^2-norm of divergences versus time (Torus).

As already mentionned, the proposed structure-preserving scheme does not guarantee divergence-free inductions. However, projecting $\underline{E}$ and $\underline{H}$ on the basis of Raviart-Thomas elements of order 1 leads to a result which is quite fair, at least non-exploding, as can be seen on Fig. 2.

Finally, in order to test the efficiency and the ease to implement PFEM, a similar simulation has been performed making use of the Python library FEniCS (Langtangen and Logg (2016)), but with a *sphere* as geometrical domain, and $\Delta t = 10^{-2}$. Here again, we can appreciate the precision of the power balance on Fig. 3 .

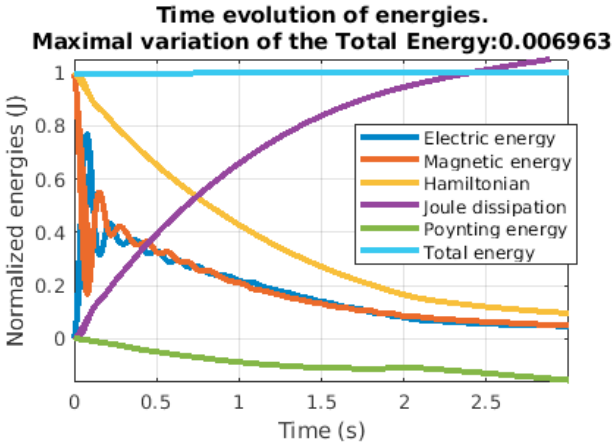

Fig. 3. Normalized energies versus time (Sphere).

4. BOUNDARY IMPEDANCE AND STRUCTURE-PRESERVING DISCRETIZATION OF THE LOSSY MODEL

Suppose that the surface $\partial\Omega$ is covered by a material, which is neither a perfect conductor, nor a perfect insulator. The boundary conditions are prescribed through a 3×3 impedance matrix, $Z(\mathbf{x})$, which acts in the tangent plane at point $\mathbf{x}$, the image of which also lies in the tangent plane; it is symmetric and positive $Z^\top = Z \geq 0$. The boundary conditions are given by: $\mathbf{E}_\tau(\mathbf{x}) = -Z(\mathbf{x})\,(\mathbf{n}(\mathbf{x}) \wedge \mathbf{H}(\mathbf{x}))$, or $\mathbf{u}_\partial(t) = -Z\,\mathbf{y}_\partial(t)$, then the energy balance (5) reads:

$$\frac{d\mathcal{E}_{em}}{dt} = -\int_{\partial\Omega} \mathbf{\Pi}\cdot\mathbf{n} = \int_{\partial\Omega} \mathbf{y}_\partial \cdot \mathbf{u}_\partial = -\int_{\partial\Omega} \mathbf{y}_\partial^\top Z\,\mathbf{y}_\partial \leq 0\,.$$

Now, following the strategy presented in Serhani et al. (2019b) for the wave equation, and making use of the structure-preserving nature of PFEM, it is straightforward to mimick these absorbing boundary conditions (ABC) at the discrete level. Using the results and notations of § 3, the impedance can be represented by a simple output feedback loop, under the form $M_\partial\,\underline{u}_\partial(t) := -\langle Z\rangle\,\underline{y}_\partial(t)$, where $\langle Z\rangle := \int_{\partial\Omega} \Psi^\top Z(\mathbf{x})\,\Psi$ is an $N_\partial \times N_\partial$ matrix, as a spatial average of the original impedance matrix on the boundary. The energy balance of the resulting closed-loop dynamical system reads:

$$\frac{d\mathcal{E}^d_{em}(t)}{dt} = -\underline{y}_\partial(t)^\top \langle Z\rangle\,\underline{y}_\partial(t) \leq 0\,,$$

proving that the closed dynamical system is dissipative.

Remark 4. Indeed, at the discrete level, the dynamical system is now of the form $M^d \frac{d\underline{\mathbf{X}}}{dt} = (J^d - R^d)\,\nabla_{\underline{\mathbf{X}}}\mathcal{E}^d_{em}$, with R^d symmetric and positive, with block matrix of size $N_m \times N_m$, $R_m := T M_\partial^{-1}\langle Z\rangle M_\partial^{-1} T^\top = R_m^\top \geq 0$, of rank N_∂, in the magnetic part, and 0 as other block matrices. This is a very nice and coherent structure result, since only those N_∂ degrees of freedom at the boundary can have some damping effect on the overall system.

5. CONCLUSION AND DISCUSSION

In this paper, the Partitioned Finite Element Method has been extended to the 3D Maxwell's equations with damping. The structure-preserving feature of the method has been fully proved and illustrated with simulations on two geometries, and run on two different FEM softwares. Moreover the boundary damping through a matrix-valued impedance has been studied and discretized adequately.

An important question remains open in this strategy about the divergences of inductions. A further investigation would be the pHDAE approach, discussed in Section 3.3.

Appendix A. VECTOR CALCULUS IDENTITIES

The first useful identity comes from two expressions to be found for $\mathbf{C}\cdot(\mathbf{E}\wedge\mathbf{H}) = \mathbf{H}\cdot(\mathbf{C}\wedge\mathbf{E}) = -\mathbf{E}\cdot(\mathbf{C}\wedge\mathbf{H})$, and applied with the derivation operator ∇, which gives in turn:

$$\text{div}\,(\mathbf{E}\wedge\mathbf{H}) = \mathbf{H}\cdot\mathbf{curl}\,\mathbf{E} - \mathbf{E}\cdot\mathbf{curl}\,\mathbf{H}\,. \tag{A.1}$$

An immediate consequence of this identity is its integral version, involving Stokes formula:

$$\int_\Omega (\mathbf{E}\cdot\mathbf{curl}\,\mathbf{H} - \mathbf{H}\cdot\mathbf{curl}\,\mathbf{E}) = -\int_{\partial\Omega}\mathbf{\Pi}\cdot\mathbf{n}\,, \tag{A.2}$$

introducing the *Poynting vector* $\mathbf{\Pi} := \gamma(\mathbf{E}\wedge\mathbf{H})$ defined on the boundary $\partial\Omega$.

Appendix B. COLLOCATED BOUNDARY CONTROLS AND OBSERVATIONS

Considering $(\mathbf{n},\tau_1,\tau_2)$ a local basis at point $\mathbf{x}\in\partial\Omega$ with $\mathbf{n}$ the outward normal to Ω, and $\tau_2 := \mathbf{n}\wedge\tau_1$, let us denote γ the trace of a vector field $\mathbf{X}$ as: $\gamma(\mathbf{X}) = X_n\mathbf{n} + X_1\tau_1 + X_2\tau_2$, and $\gamma_n(\mathbf{X}) := \mathbf{n}\cdot\gamma(\mathbf{X}) = X_n$ the *normal* trace.
Then $\mathbf{n}\wedge\gamma(\mathbf{X}) = -X_2\tau_1 + X_1\tau_2$, and

$$(\mathbf{n}\wedge\gamma(\mathbf{X}))\wedge\mathbf{n} = X_1\tau_1 + X_2\tau_2 := \gamma_\tau(\mathbf{X}),$$

the *tangential* trace. Hence, the previous quantity $\mathbf{n}\wedge\gamma(\mathbf{X})$ will be called the *rotated* tangential trace.

Since $\mathbf{n}\cdot(\mathbf{E}\wedge\mathbf{H}) = \mathbf{H}\cdot(\mathbf{n}\wedge\mathbf{E}) = -\mathbf{E}\cdot(\mathbf{n}\wedge\mathbf{H})$, one can define different collocated inputs-outputs for boundary control purposes, the equality to be fulfilled being

$$\int_{\partial\Omega}\mathbf{u}_\partial\cdot\mathbf{y}_\partial = -\int_{\partial\Omega}\mathbf{\Pi}\cdot\mathbf{n}\,. \tag{B.1}$$

In practise, a first possible choice is $\mathbf{u}_\partial := \gamma_\tau(\mathbf{E})$ the tangential trace of the electric field, and $\mathbf{y}_\partial := \mathbf{n}\wedge\gamma(\mathbf{H})$, the rotated tangential trace of the magnetic field.

Alternatively, a second possible choice is $\mathbf{u}_\partial := \gamma_\tau(\mathbf{H})$ the tangential trace of the magnetic field, and $\mathbf{y}_\partial := -\mathbf{n}\wedge\gamma(\mathbf{E})$, the rotated tangential trace of the electric field.

REFERENCES

Beattie, C., Mehrmann, V., Xu, H., and Zwart, H. (2018). Linear port-Hamiltonian descriptor systems. *Mathematics of Control, Signals, and Systems*, 30(4), 1–27.

Brugnoli, A., Alazard, D., Pommier-Budinger, V., and Matignon, D. (2019a). Port-Hamiltonian formulation and symplectic discretization of plate models Part I: Mindlin model for thick plates. *Applied Mathematical Modelling*, 75, 940–960.

Brugnoli, A., Alazard, D., Pommier-Budinger, V., and Matignon, D. (2019b). Port-Hamiltonian formulation and symplectic discretization of plate models Part II: Kirchhoff model for thin plates. *Applied Mathematical Modelling*, 75, 961–981.

Cardoso-Ribeiro, F.L., D., M., and Lefèvre, L. (2019). A Partitioned Finite-Element Method (PFEM) for power-preserving discre tization of open systems of conservation laws. *arXiv:1906.05965*. Under revision.

Cardoso-Ribeiro, F.L., Matignon, D., and Lefèvre, L. (2018). A structure-preserving Partitioned Finite Element Method for the 2D wave equation. In *IFAC-PapersOnLine*, volume 51(3), 119–124. 6th IFAC Workshop on Lagrangian and Hamiltonian Methods for Nonlinear Control (LHMNLC).

Duindam, V., Macchelli, A., Stramigioli, S., and Bruyninckx, H. (2009). *Modeling and Control of Complex Physical Systems: The Port-Hamiltonian Approach*. Springer-Verlag Berlin Heidelberg.

Eberard, D., Maschke, B., and van der Schaft, A. (2007). On the interconnection structures of discretized port hamiltonian systems. *Proceedings in Applied Mathematics & Mechanics*, 7(1), 3030005–3030006. doi:10.1002/pamm.200700422.

Farle, O., Klis, D., Jochum, M., Floch, O., and Dyczij-Edlinger, R. (2013). A port-Hamiltonian finite-element formulation for the Maxwell equations. In *2013 International Conference on Electromagnetics in Advanced Applications (ICEAA)*, 324–327.

Haine, G., Matignon, D., and Anass, S. (2020). Numerical analysis of a structure-preserving space-discretization for an anisotropic and heterogeneous boundary controlled N-dimensional wave equation as port-Hamiltonian system. Submitted.

Hecht, F. (2012). New development in FreeFem++. *Journal of Numerical Mathematics*, 20(3–4), 251–265.

Kotyczka, P. (2019). *Numerical Methods for Distributed Parameter Port-Hamiltonian Systems*. TUM.University Press, Munich. Habilitation.

Langtangen, H.P. and Logg, A. (2016). *Solving PDEs in Python: The FEniCS Tutorial I*. Number 3 in Simula SpringerBriefs on Computing. Springer International Publishing.

Monk, P. (2003). *Finite element methods for Maxwell's equations*. Numerical Mathematics and Scientific Computation. Oxford University Press, New York.

Payen, G., Matignon, D., and Haine, G. (2018). Simulation of plasma and Maxwell's equations using the port-Hamiltonian approach. URL `http://oatao.univ-toulouse.fr/22823/`. Internship report.

Serhani, A., Matignon, D., and Haine, G. (2019a). A Partitioned Finite Element Method for the Structure-Preserving Discretization of Damped Infinite-Dimensional Port-Hamiltonian Systems with Boundary Control. In Nielsen, Frank and Barbaresco, Frédéric (eds.), *Geometric Science of Information*, volume 11712 of *Lecture Notes in Computer Science*, 549–558. Springer International Publishing.

Serhani, A., Matignon, D., and Haine, G. (2019b). Partitioned Finite Element Method for port-Hamiltonian systems with Boundary Damping: Anisotropic Heterogeneous 2D wave equations. In *IFAC-PapersOnLine*, volume 52(2), 96–101. 3rd IFAC workshop on Control of Systems Governed by Partial Differential Equations (CPDE).

van der Schaft, A.J. and Maschke, B. (2002). Hamiltonian formulation of distributed-parameter systems with boundary energy flow. *Journal of Geometry and Physics*, 42(1–2), 166–194.

Vu, N.M.T. (2014). *Port-Hamiltonian approach for modelling, reduction and control of plasma dynamics in Tokamaks*. Ph.D.thesis, Université de Grenoble.

Vu, N.M.T., Lefèvre, L., and Maschke, B. (2012). Port-Hamiltonian formulation for systems of conservation laws: application to plasma dynamics in Tokamak reactors. In *IFAC Proceedings Volumes*, volume 45(19), 108–113. 4th IFAC Workshop on Lagrangian and Hamiltonian Methods for Non Linear Control (LHMNLC).

Vu, N.M.T., Lefèvre, L., and Maschke, B. (2016). A structured control model for the thermo-magneto-hydrodynamics of plasmas in Tokamaks. *Mathematical and Computer Modelling of Dynamical Systems*, 22(3), 181–206.

Weiss, G. and Staffans, O.J. (2013). Maxwell's equations as a scattering passive linear system. *SIAM Journal on Control and Optimization*, 51(5), 3722–3756.